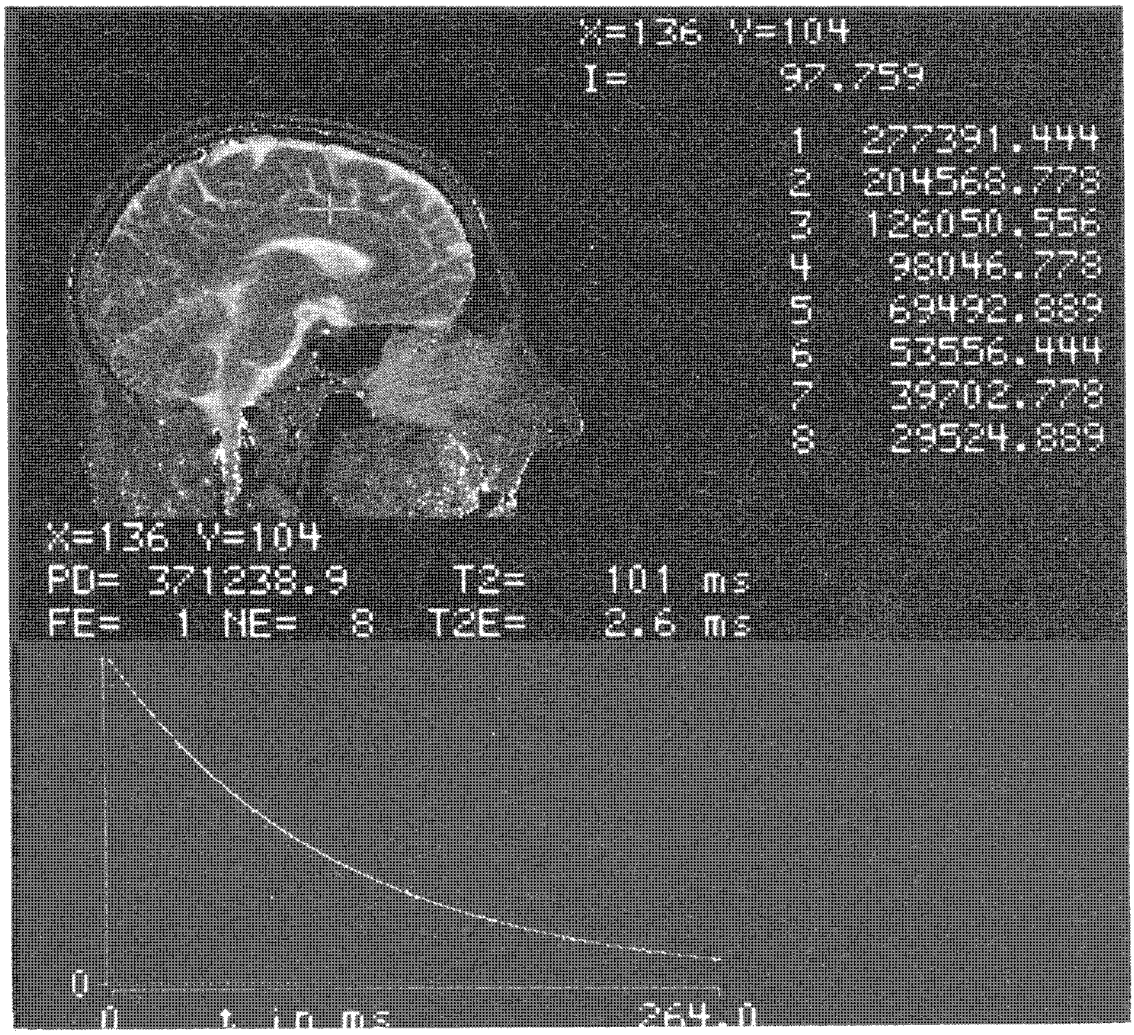

Estimation of the spin-spin relaxation times T_2. The diagram shows the intensities (signal amplitudes) of the 8 individual echoes for the location indicated by the cross. By moving the cross over the image, the spin-spin relaxation time can be obtained at any point of the image.

Figure 6.35 Estimation of the spin-spin relaxation time at each position within the slice through the skull of Figure 6.32 .

6.9.2 Chemical shift anisotropy.

The NMR resonances depend on the chemical environment of a nucleus. This environment is different in each direction in space. However, in solution NMR experiments, the molecules usually tumble and rotate rapidly in space, a motion which is usually faster than the time required for NMR transitions. The differences in the chemical environment along each coordinate in space become only apparent, if molecules are aligned with a preferred direction in space (relative to the magnetic field B_0). An example for such an alignment are the lipid molecules in a lipid bilayer which is supported for example by a glass plate (or by a germanium

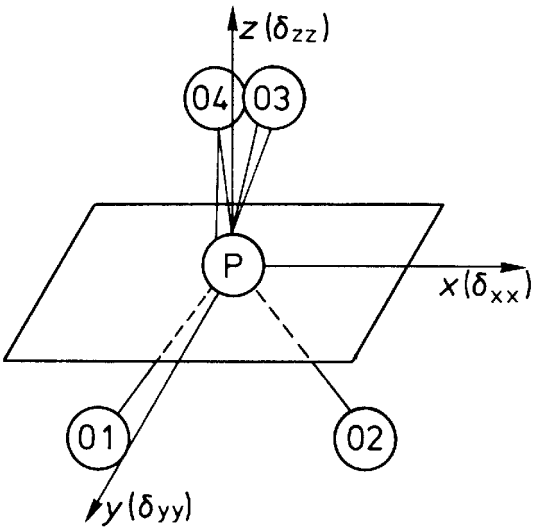

Anisotropy of the chemical environment and the chemical shift of ^{31}P in the phosphate group of a phospholipid. O3 and O4 are the free oxygenes and 02 and 01 the oxygens in the ester bonds. [After Seelig, J. (1978), Biochim. Biophys. Acta 515, 105].

Figure 6.36 Anisotropy of the chemical shifts of ^{31}P in the phosphate group of a phospholipid.

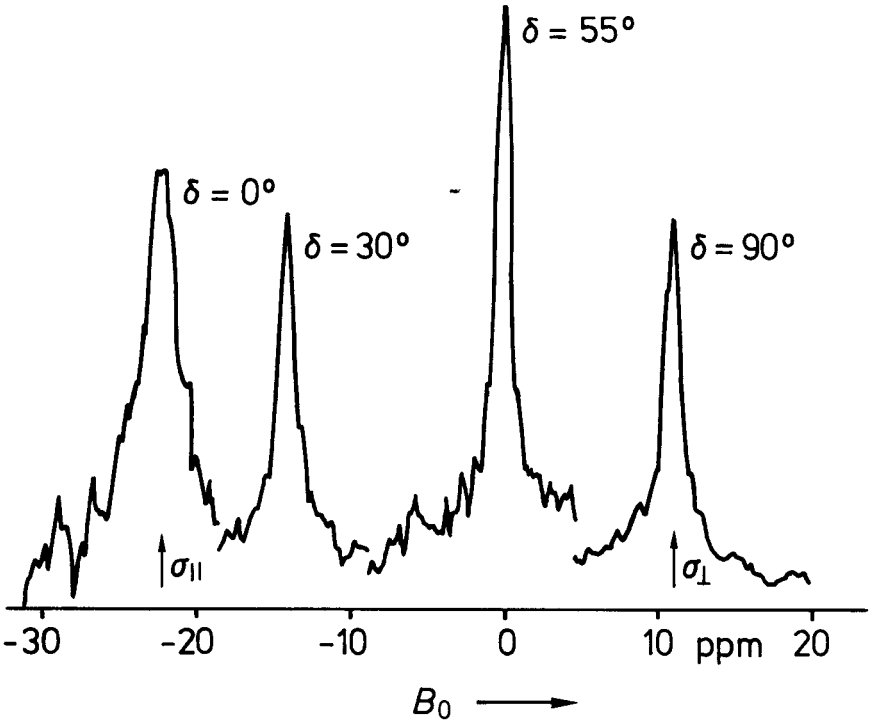

^{31}P-NMR spectra of oriented samples of a phospholipid in planar lipid multilayers. δ is the angle between the magnetic field B_0 and the membrane normal. [After Seelig, J. Gally, H. (1976), Biochemistry 15, 5199]

Figure 6.37 Chemical shifts of ^{31}P in spatially oriented phospholipids.

plate). The differences in the chemical environment of the ^{31}P nucleus of the phosphate group are shown in Figure 6.36. If the lipids are oriented with their molecular long axis in x, y, and z-direction (relative to the field B_0, which is in z-direction), different chemical shifts of the ^{31}P nucleus are observed (which is a consequence of the different electron density of the phosphate group in a phospholipid in each direction in space).

If phospholipid molecules are not oriented in space, there are many cases in which these molecules are still not allowed to tumble and rotate freely. For example, their motions can be restricted by the supramolecular structure of the lipid-bilayer. Thus, phospholipid NMR-spectra are powder pattern spectra that consist of a superposition of the NMR spectra of all molecules with different orientations in space. Such spectra are shown for different lipid phases in Figure 6.38. ^{31}P-NMR spectroscopy is therefore a tool to determine supramolecular structure.

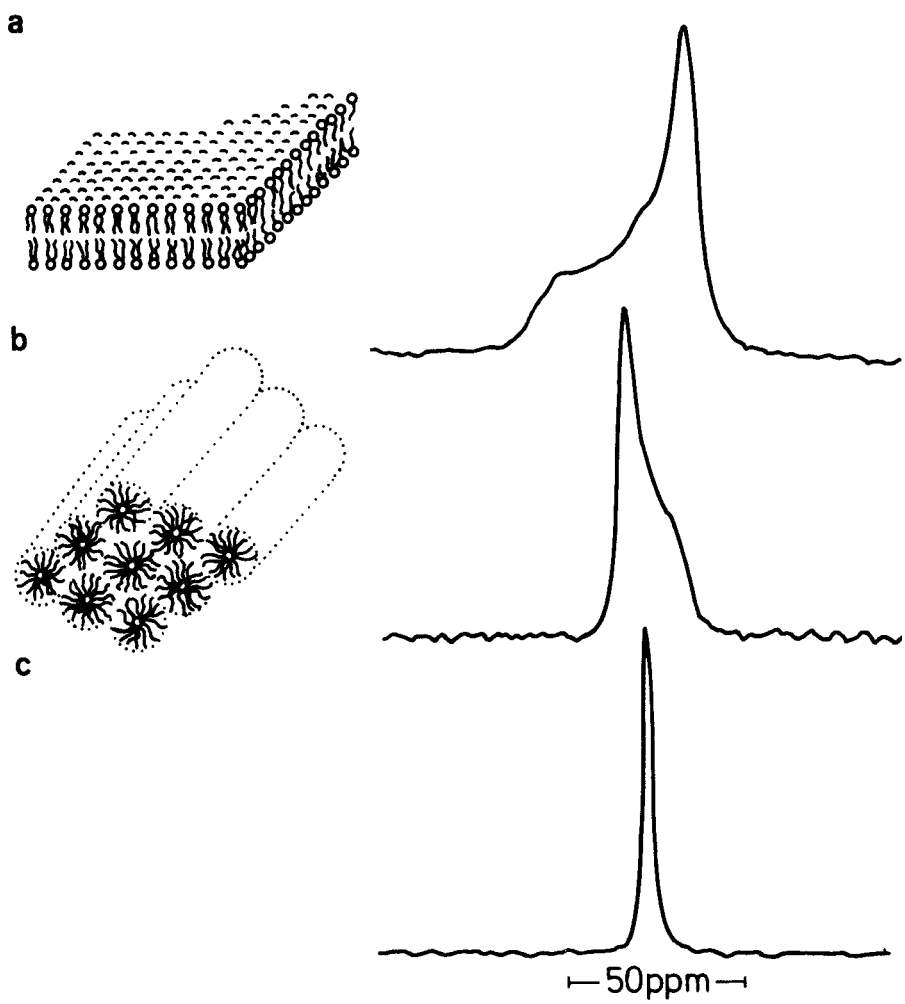

^{31}P-NMR spectra of different phases of hydrated phospholipids. ***a*** phospholipid bilayer, ***b*** hexagonal phase, ***c*** isotropic micellar phase. [After Cullis, P.R., Hoppe, M.J. (1978), Nature 271, 672].

Figure 6.38 31P-NMR spectra of different lipid phases.

6.9.3 Intensity gain by selective population inversion.

The modest sensitivity of the resonances of many nuclei is a major problem in NMR spectroscopy. The reason is the small difference in the population of the different energy levels (see section 6.7.1). The peak intensity is proportional to the difference of the populations of the to energy levels, n_h-n_l, between which the transition takes place. The ratio of the two populations is given by a Boltzmann relation:

$$\frac{n_h}{n_l} = \exp\left(-\frac{\Delta E}{kT}\right) = \exp\left(-\frac{g_N \beta_N B_0}{kT}\right) = \exp\left(-\frac{g_N \gamma \hbar B_0}{kT}\right) \approx 1 - \frac{g_N \gamma \hbar B_0}{kT}$$

Eq. 6.28

The difference between these two energy levels is the larger the larger the magnetic field B_0. This is one of the reasons why the development of new NMR spectrometers aims to increase the magnetic field strength.

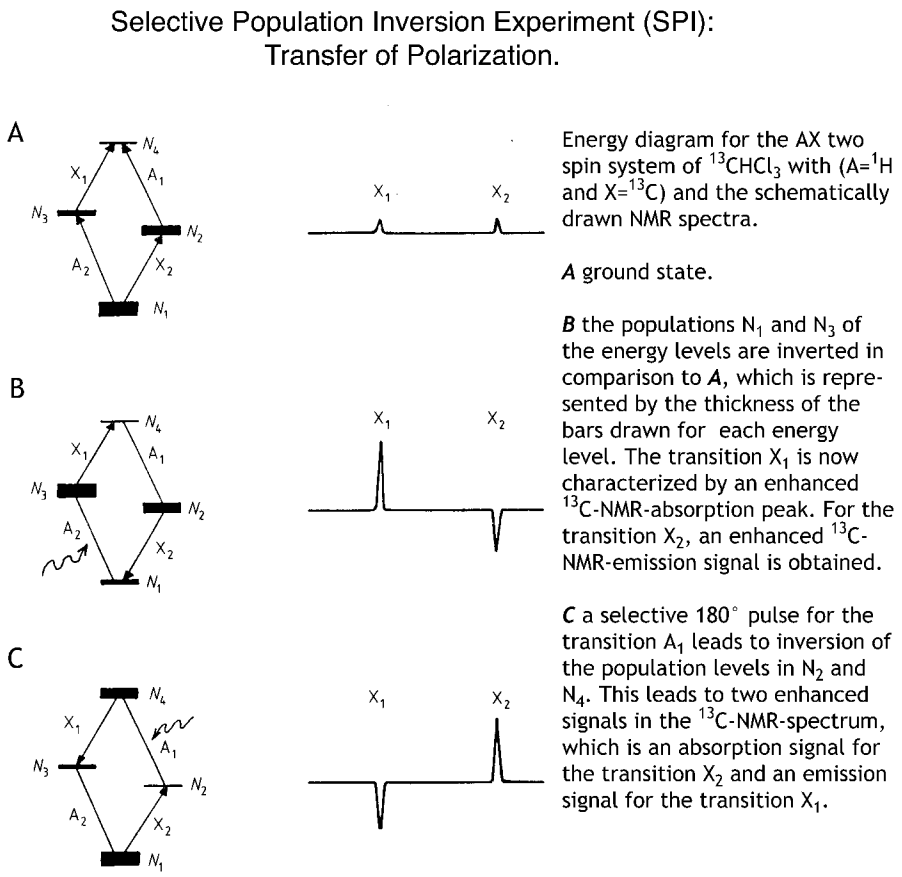

Figure 6.39 Schematic diagram of a polarization transfer experiment, here that of a selective population inversion experiment (SPI).

However, the population difference and thus the signal strength, is also dependent on the magnetogyric ratio γ. Nuclei like ^{1}H, ^{19}F, and ^{31}P have a large g and are therefore better detectable than nuclei such as ^{13}C, ^{15}N and ^{2}H. In addition, the less sensitive nuclei are often also less abundant in nature, which is an additional disadvantage. Special experiments with selective pulses increase the intensity of the NMR absorption peaks. One example of such experiments is the selective population inversion experiment (SPI). To illustrate the experiment, chloroform $^{13}CHCl_3$ shall be considered. The ^{13}C NMR spectrum consists of a doublet, due to coupling between the spin of the ^{13}C (spin 1/2) and the spin of the ^{1}H (J(C,H) = 209 Hz). Would the ^{1}H broad band decoupler be turned on, only one signal would be observed. The spectrum is depicted in Figure 6.39***A***. The transitions of the protons A_1 and A_2 are observed in the ^{1}H-NMR spectrum as satellites of the main signal, if normal Chloroform (containing mostly ^{12}C) is used. The populations N_1 to N_4 of the 4 possible different energy levels is again given by Boltzmann distributions (Eq. 6.28). Eq. 6.28 allows to deduce the relative populations of the energy levels N_1 to N_4, and therefore the signal intensities of the corresponding transitions. To estimate the relative populations, one must consider that the magnetogyric ratio of ^{1}H is about four times larger than that of ^{13}C. The differences between N_1 and N_2 and also between N_3 and N_4 are small, because they are determined by the magnetogyric ratio of ^{13}C. In contrast, the differences between N_1 and N_3 and between N_2 and N_4 are larger, because these differences are determined by the magnetogyric ratio of the proton. Thus the energy levels N_1 and N_2 are stronger populated than the energy levels N_3 and N_4. A selective 180°pulse to induce a transition A_2 will invert the population ratio between levels 1 and 3. Now, N_3 is larger than N_1 , Figure 6.39 ***B***. For the transitions X_1 and X_2, the situation has now changed: the intensity of the NMR peak corresponding to the transition X_1 will now increase, because the difference between the populations of N_3 and N_4 was increased due to the transfer of magnetization (polarization). For the transition X_2 we now have an increased difference between N_2 and N_1 (with $N_2 > N_1$!). The signal intensity is also increased for this transition, but an emission is observed. Similar considerations may be made for a selective 180° pulse to induce a transition A_2. Such a pulse inverts the populations of levels 2 and 4. For X_1 an increased emission and for X_2 an increased absorption signal are observed (Figure 6.39 ***C***). The signal amplification depends on the ratio of the magnetogyric ratios of the nuclei:

$$1+\frac{\gamma_A}{\gamma_X} \qquad \text{Eq. 6.29}$$

and

$$1-\frac{\gamma_A}{\gamma_X} \qquad \text{Eq. 6.30}$$

In case of chloroform ($\gamma(^{1}H) / \gamma(^{13}C) = 4$), the signal intensity is 5 times larger than normal and the emission signal is 3 times larger. Because of the selective inversion of the population ratios, this method is called selective population inversion experiment (SPI). The selective population inversion experiment is an example for polarization transfer. Today, the SPI experiment has been superseded by other techniques, i.e. INEPT (insensitive nuclei enhanced by polarization transfer) and DEPT (distortionless enhancement by polarization transfer) experiments.

6.10. 2-dimensional NMR spectroscopy.

In conventional 1-dimensional NMR spectroscopy signal intensities are given as a function of a chemical shift, i.e. ppm of magnetic field or frequency units. In other words the signal is dependent on the position along one axis. In two-dimensional NMR spectroscopy signals are obtained in dependence of two frequencies and the signal intensity is then plotted in the third dimension. Different kinds of 2-dimensional NMR spectra are distinguished. For example, if chemical shifts are represented by one axis and coupling constants are represented on the second axis the spectra are called 2-dimensional J-resolved NMR spectra. However, if chemical shifts are plotted on both axes, the spectra are called correlated 2-dimensional NMR spectra. Examples for the latter are spectra with ^{1}H chemical shifts on both axes, (H, H)-COSY, or spectra with ^{1}H chemical shifts on one axis and ^{13}C chemical shifts on the other axis, (H,C)-COSY. Some different types of two dimensional NMR methods are listed in Table 4.

Experiment	Nucleus	Information
Heteronuclear J-coupled 13C NMR	^{13}C	C,H coupling constants
Homonuclear J-coupled 1H-NMR	^{1}H	Estimation of chemical shifts in complex spectra
(H,C) -COSY, correlated spectroscopy	^{1}H, ^{13}C	Assignment of signals in 1H and 13C-NMR spectra from known signals
(H,H)-COSY, correlated spectroscopy	^{1}H	Assignment in complex spectra
H-Relayed-(H,C) COSY	^{1}H, ^{13}C	Assignments of non-scalar coupled nuclei
H-Relayed-(H,H) COSY	^{1}H	Assignment of non-scalar coupled protons
Inverse (C,H) -COSY	$^{13}C/^{1}H$	Assignments of non-scalar coupled nuclei
Exchange Spectroscopy		
NOESY	^{1}H	Proof of exchange, Proof of spatial neighborhood of nuclei
2D-INADEQUATE	^{13}C	Assignment of coupled 13C nuclei

Table 4 Some 2-D NMR experiments

How are such two-dimensional spectra obtained ? Two dimensional spectra require the coupling of nuclear dipoles. In must not necessarily be indirect of J-coupling but can also be through

space coupling of nuclei. The through space coupling that makes use of the nuclear overhouser effect between magnetic dipoles offers an opportunity to study the three-dimensional structure of molecules by nuclear overhouser effect spectroscopy (NOESY). Two illustrate some principles of 2-D NMR spectroscopy we will focus on the ^{1}H and ^{13}C nuclei. In principle the same methods can also be applied to other nuclei.

6.10.1 The 2-dimensional NMR experiment.

In a normal FT-NMR experiment the detection phase immediately follows the excitation of the spin system and the free induction decay is recorded. In 2-D NMR spectroscopy, pulse sequences are more complex and the spin system is “prepared” before the FID is recorded. In addition, the two phases “preparation” and “detection” are extended by a third phase, the evolution phase, in which the spins can couple with each other. The time of this evolution phase is kept variable and two Fourier transformation can now be applied to yield a signal intensity as a function of frequencies that arise from Fourier transformation in the domain of the evolution time and from a Fourier transformation in the domain of the detection time.

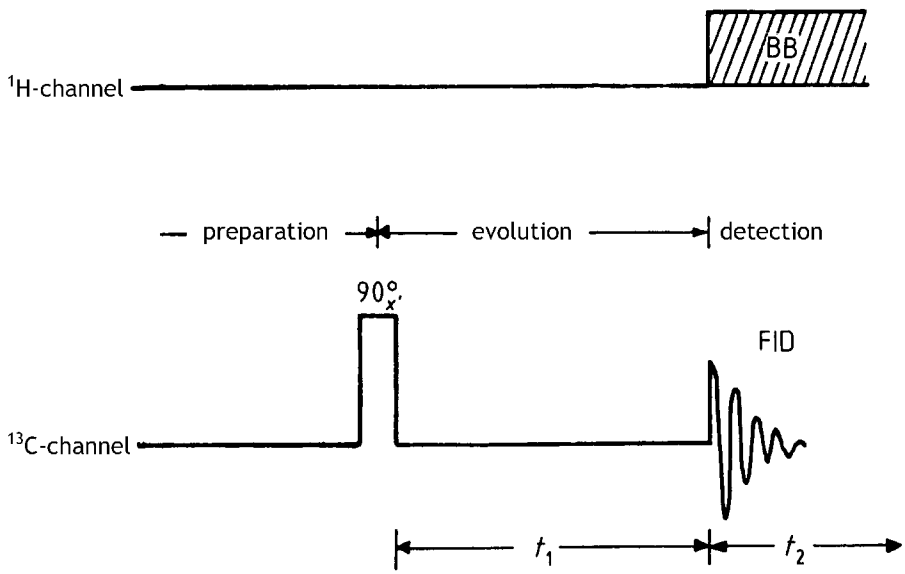

Principle of a 2-dimensional ^{13}C-NMR experiment. The time t_1 is a variable. The second variable is the time t_2. In the time t_1 the spin-system is allowed to "develop".

Figure 6.40 Principle of a 2-dimensional NMR experiment.

To understand the concept behind the 2-D spectroscopy we perform a simple experiment. We consider a simple 2 spin system AX with A=^{1}H and X=^{13}C. In contrast to a conventional experiment, we introduce a delay time, t_1, between the preparation of the spin system (which is performed by a 90°x'-pulse, and the acquisition of the free induction decay during a time t_2. In addition the ^{1}H-broad band decoupler shall only be switched on during the detection of the free induction decay (Figure 6.40). We assume that we perform n experiments with different t_1 values, starting with t_1=0. The time t_1 shall be increased from experiment to experiment by a few ms. The Fourier transformation (FT) of the n interferograms with respect to t_2 results in n different NMR spectra, which consist of a singlet, since during the acquisition of the FID, the ^{1}H-BB decoupler is turned on. If the broad band decoupler was turned on also during t_1, the spectra would be all the same except of a decreasing intensity caused by relaxation during t_1. Since the broad band decoupler was only turned on during the detection phase t_2, the ^{13}C nuclei and the protons are coupling in the evolution phase. The vector diagrams shown in Figure 6.41 demonstrate how this C,H coupling affects the singlet in the spectrum. After the 90 $°_{x'}$ pulse, the macroscopic magnetization of the ^{13}C nuclei is in direction of y'. The magnetization M_C of the ^{13}C nuclei is split into two parts, $M_C^{H\alpha}$ and $M_C^{H\beta}$, that correspond to the ^{13}C nuclei in chloroform molecules with a proton of spin α and spin β, respectively. The two vectors, $M_C^{H\alpha}$ and $M_C^{H\beta}$, precess with different Larmor frequencies:

$$M_C^{H_\alpha} = \nu_C - \frac{1}{2}J(\mathrm{C,H}) \qquad \text{and}$$
$$M_C^{H_\alpha} = \nu_C + \frac{1}{2}J(\mathrm{C,H}) \qquad \text{Eq. 6.31}$$

Assumed that the coordinate system, x',y', rotates with the average of the Larmor frequency, ν_C, one vector rotates faster, the other slower, each by J(C,H) / 2. The rotations of the two vectors are indicated by small arrows in Figure 6.41 . During the time t_1, the two vectors of magnetization, $M_C^{H\alpha}$ and $M_C^{H\beta}$, will travel the angles ϕ_α and ϕ_β according to

$$\varphi_\alpha = 2\pi\left(\nu_C - \frac{1}{2}J(\mathrm{C,H})\right)t_1 \qquad \text{and}$$
$$\varphi_\beta = 2\pi\left(\nu_C + \frac{1}{2}J(\mathrm{C,H})\right)t_1 \qquad \text{Eq. 6.32}$$

The phase difference between the two vectors can now be calculated according to

$$\Theta = \varphi_\beta - \varphi_\alpha = 2\pi \cdot J(\mathrm{C,H}) \cdot t_1 \qquad \text{Eq. 6.33}$$

After t_1=[4 J(C,H)]$^{-1}$ (which is in the ms region), the phase difference between the two vectors is 90°, after t_1=[2 J(C,H)]$^{-1}$ the difference is 180°, and after t_1=[J(C,H)]$^{-1}$ the two vectors are in phase again, but their vectors now point into the –y' direction. How do the

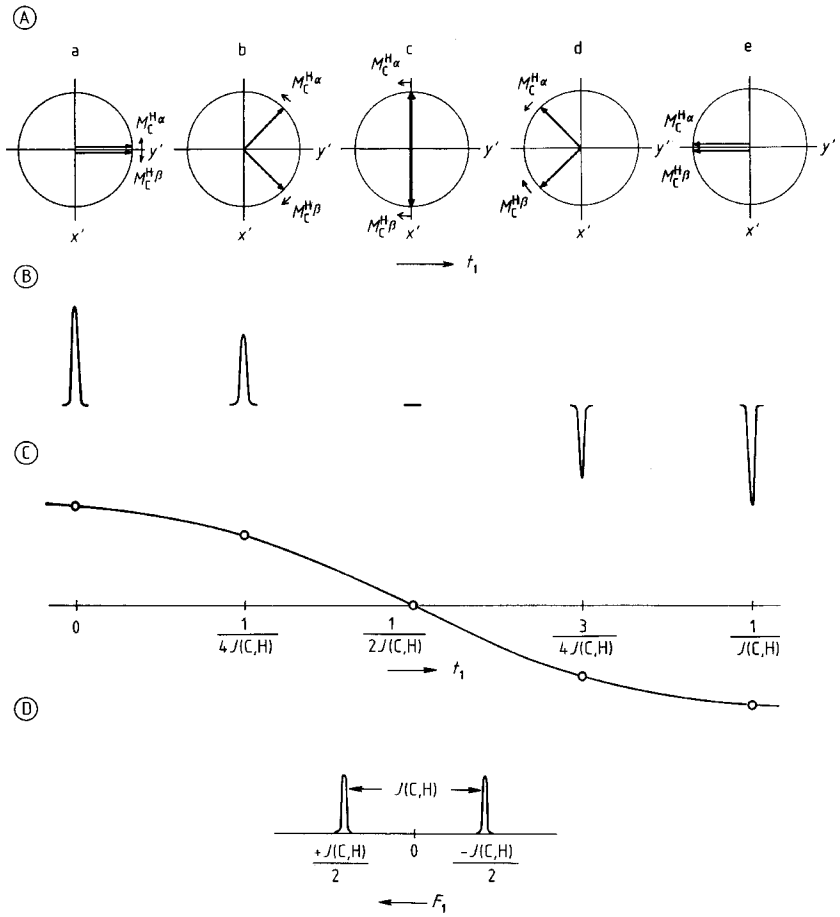

A Vector diagrams for the ^{13}C magnetization vectors of a AX two spin-system (A=^1H and X=^{13}C) at different times t_1. The coordinate system x', y', z rotates around z with the Larmor frequency ν_C. (***a*** t_1=0, ***b*** t_1=[4 J(C,H)]$^{-1}$, ***c*** t_1=[2 J(C,H)]$^{-1}$, ***d*** t_1=3 [4 J(C,H)]$^{-1}$, ***e*** t_1=[J(C,H)]$^{-1}$).

B The ^{13}C NMR spectrum consists of singlets after a Fourier transformation with respect to t_2 (with ^1H BB decoupling). The amplitudes of the singletts depend on t_1.

C The amplitude is modulated by J(C,H)

D By Fourier transform with respect to t_1, two signals are obtained with a distance of J(C,H) on the frequency axis F_1.

Figure 6.41 Vector diagrams for the magnetization vectors of ^{13}C in an AX two spin system.

frequency spectra look like ? Since the BB decoupler is turned on during the detection of the FID, all C, H -coupling is eliminated during this phase, and the F_2 spectra consist of singlets only. However the interaction between the nuclei during the time t_1 remains unaffected. To understand the t_1 effect, we consider the state of the system after a time t_1= [4 J(C,H)]$^{-1}$, when the phase difference is 90°. Switching on the BB decoupler eliminates the source for the different precession frequencies of $M_C^{H\alpha}$ and $M_C^{H\beta}$. Now, both rotate equally fast with an average Larmor frequency ν_C. However, their phase difference of 90 ° remains the same. The detector detects a signal with an amplitude that is proportional to the sum of the two vectors,

$M_C^{H\alpha}$ and $M_C^{H\beta}$. At t_1=0, both vectors are parallel, the sum of the vectors is largest and the amplitude of the signal has a maximum. At t_1= [2 J(C,H)]$^{-1}$ the component in y' direction is 0 and a signal cannot be detected. At t_1= [J(C,H)]$^{-1}$, the signal is as large as at t_1= 0, except for a loss due to relaxation, but it will have a negative amplitude. The signals that are obtained at different times t_1 are shown in Figure 6.41 B. The amplitude of the signal as a function of time is shown in Figure 6.41 C. A second Fourier transform with respect to time t_1 will thus yield two frequencies that differ by the coupling constant J. The F_2 spectrum thus contains the chemical shifts d and the F_1 spectrum the coupling constants J(C,H). In case of chloroform, all F_2 spectra consist of a singlet, whereas the F_1 spectrum consists of a dublet with a distance equal to the coupling constant (Figure 6.42).

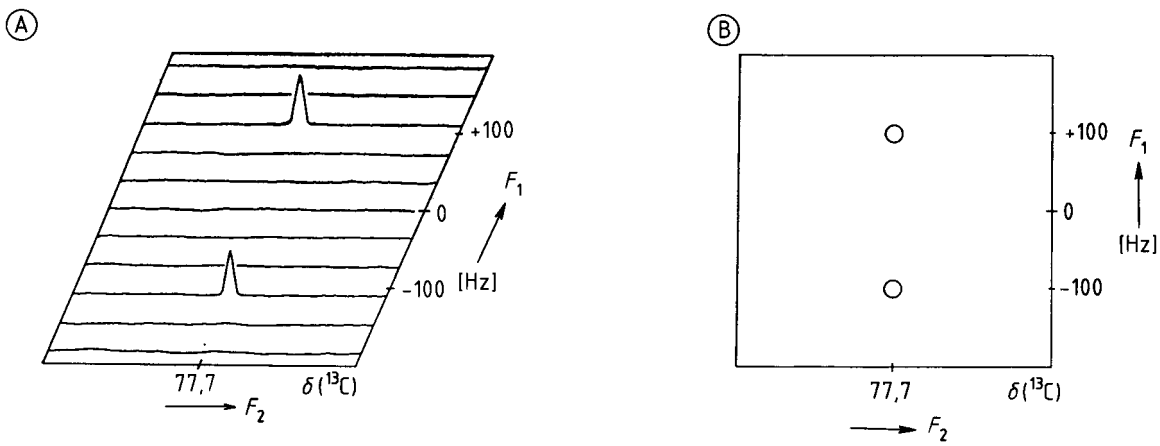

Schematic representation of a 2-D spectrum. ***A*** stacked plot. The F_2 -axis corresponds to the normal frequency axis with the δ-scale of the 1-D NMR spectrum. F_2 spectra are stacked for different F_1 values.
B Contour plot. The contour plot is a slice through the stacked plot at a defined signal height. (Note that in the stacked plot, spectra are offset in F_1 direction to improve readability.

Figure 6.42 Schematic representation of a 2-D spectrum.

6.10.1.1 Two-dimensional J-resolved NMR spectroscopy.

In the experiment that was discussed in the last section, two Fourier transformations were performed that gave rise to a two dimensional spectrum. In such a spectrum, the chemical shifts were given in one dimension (F_2-axis) and the C,H-coupling constants were given in the second dimension (F_1-axis). Since the coupling took place between hetero nuclei, we discussed the simplest case of a heteronuclear 2-dimensional J-resolved NMR spectroscopy (J, δ-spectroscopy). There are different variants of this kind of 2-D spectroscopy, from which the so-called gated decoupling method shall be discussed. The pulse sequence of this method is given in Figure 6.43 To understand the effect of the pulse sequence, we shall again

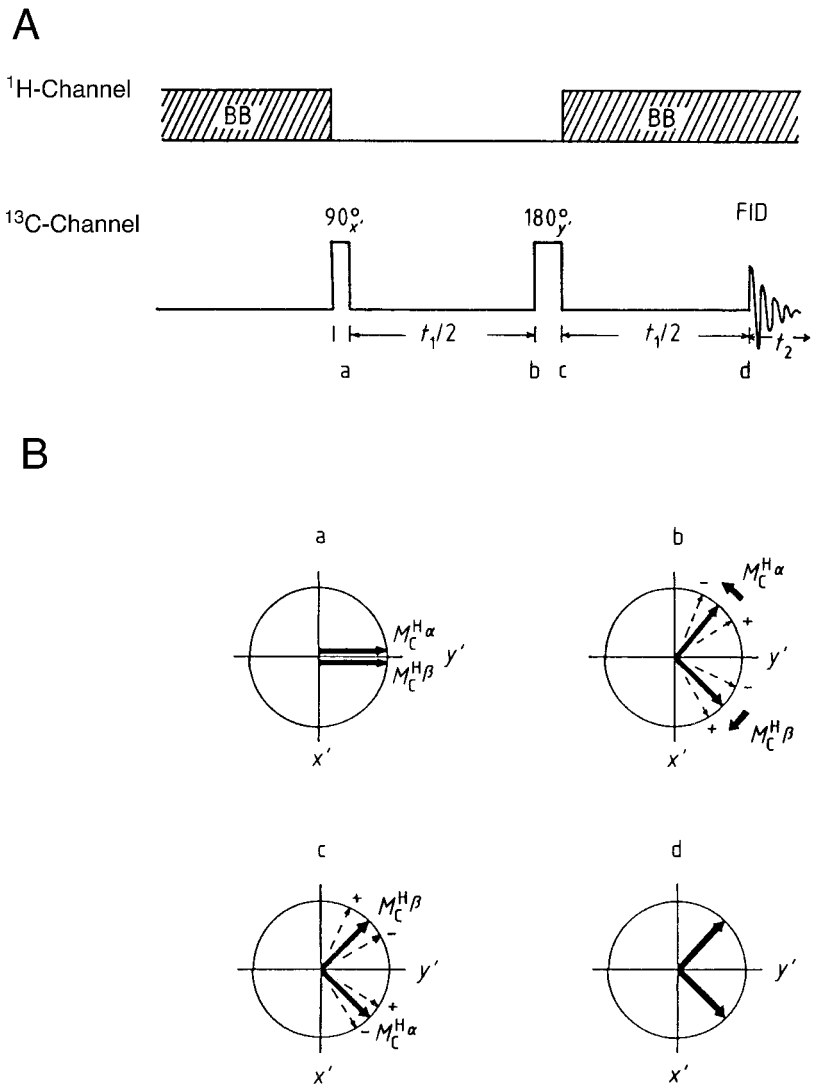

Heteronuclear two-dimensional *J*-resolved ^{13}C-NMR spectroscopy. ***A*** Pulse sequence. ***B*** Evolution of the transversal ^{13}C magnetization vectors M_C for an AX-two-spin system. with A=^{1}H and X=^{13}C in a rotating coordinate system (x',y'-plane). $M_C^{H\alpha}$ and $M_C^{H\beta}$ correspond to the ^{13}C magnetization vectors for the molecules with a proton in the α or in the β state, respectively. Diagrams in ***B*** are drawn corresponding to the times a, b, c, and d indicated in ***A***. The spin-system is developing with the coupling constant *J*(C, H) and is partially dispersed because of field inhomogeneities (slower and faster than average precession of the spins is indicated by + and -). In practice, the broad-band decoupler is switched on in the first half of the evolution phase ($t_1/2$) and during detection.

Figure 6.43 Heteronuclear 2-D J-resolved ^{13}C-NMR spectroscopy . Pulse Sequence and development of the spin-system.

consider the AX two spin system of chloroform ($^{13}CHCl_3$). The basis for this experiment is the pulse sequence $90°_{x'}$—t—$180°_{y'}$—t (echo). Compare to the pulse sequence given in Figure 6.40 this sequence now has a $180°_{y'}$ pulse in y-direction after half of the evolution time $t_1/2$. In addition, the new sequence also has the broad band decoupler turn on during the second half of the evolution time. To illustrate the behavior of the spin system, vector diagrams are drawn in Figure 6.43B. The coordinate system x', y', and z again rotates with

the mean frequency ν_C. The first pulse 90°x‘ in x‘-direction rotates the two magnetization vectors $M_C^{H\alpha}$ and $M_C^{H\beta,}$ to the y‘-axis. During $t_1/2$ ms the two vectors will separate and $M_C^{H\beta,}$ is the vector that rotates faster and $M_C^{H\alpha}$ the vector that rotates slower. In the diagram (Figure 6.43 B), the arrows indicate the relative directions of motion. Due to field inhomogeneities, the motions will be partially disperse either faster or slower than average. A $180°_{y'}$ pulse in y-direction will mirror the spins with respect to the y‘ axis (Figure 6.43 C). After an additional time of $t_1/2$ ms, the spins would be refocused in the y‘-axis, if the ^1H broad-band decoupler were turned off. However, if the broad band decoupler is turned on during the second $t_1/2$ ms, the vectors $M_C^{H\alpha}$ and $M_C^{H\beta,}$ will now rotate equally fast (with ν_C, which is the speed of the coordinate system), but their phase difference will remain the same.

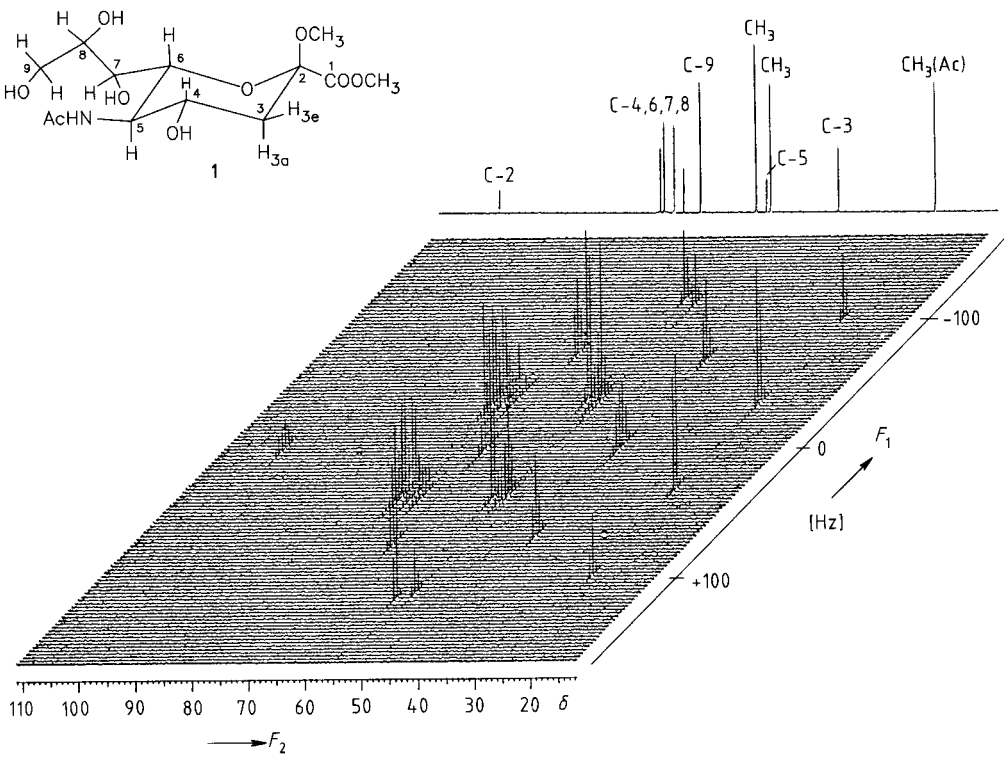

Stacked plot of the heteronuclear *J*-coupled 100.6 MHz ^{13}C NMR spectrum. On the upper edge, the projection of the multiplets is shown. This spectrum corresponds to the ^1H BB-decoupled ^{13}C NMR spectrum. Multiplets parallel to the F_1-axis indicate how many H-atoms are bound to the corresponding carbon atom. The distance between the signals in the multipletts corresponds to *J*(C,H)/2, since the spin-system developed for 0.5 t_1 ms. Signals of the quarternary C-atoms of the carboxy and of the acetamide-group are not shown.

Figure 6.44 Heteronuclear J-coupled 2D-NMR spectrum of neuraminic acid.

The partial dispersion of the spins that are caused by field inhomogeneities, however, is

equalized after $t_1/2$ ms by the $180°_{y'}$ -pulse. After a time t_1, the signal may be recorded. This signal is proportional to the sum of the two vectors, $M_C^{H\alpha}$ and $M_C^{H\beta}$. This sum depends on the phase difference, which is again dependent on the coupling constant J(C,H). The ^{13}C-NMR signal is thus modulated by J(C,H). The Fourier transformation with respect to t_2 results in a singlet that is modulated by J(C,H). The Fourier transformation with respect to t_1 results in a doublet on the F_1-axis that has a distance of 1/2 J(C,H) (the system was allowed to develop only $t_1/2$).

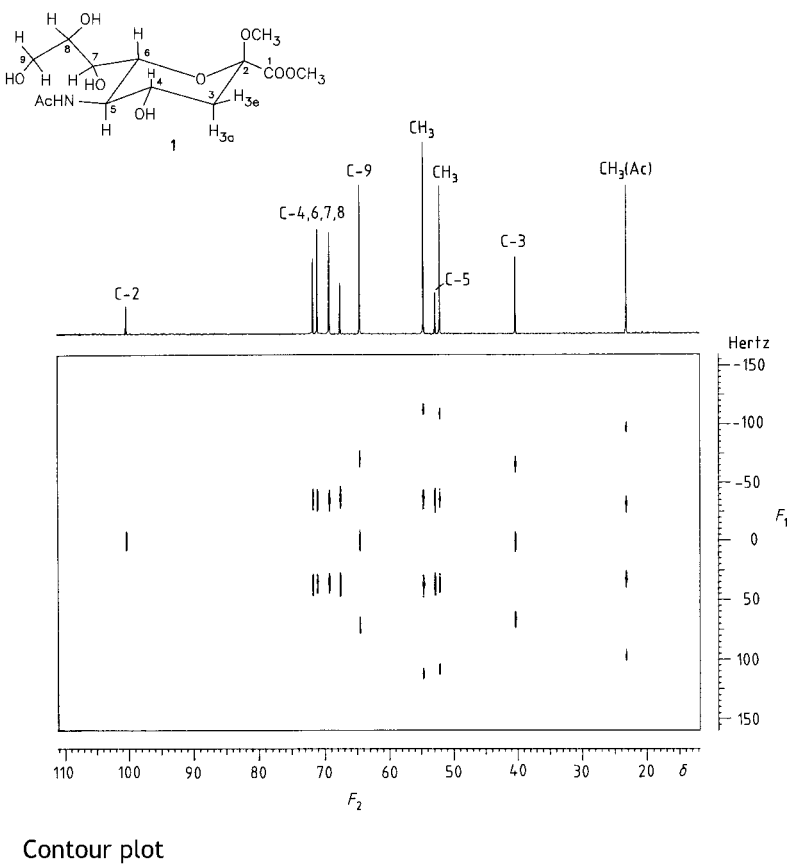

Figure 6.45 Contour plot of the spectrum shown in Figure 6.44

For other molecules, the F_2 spectrum will consist of as many singlets as there are different ^{13}C-atoms. On the t_1-scale, all signals are modulated with the corresponding C,H-coupling constants. Parallel to the F_1 axis, the multiplets are obtained, that result from the coupling with the protons: singlets for quarternary carbons, doublets for C-H (tertiary carbons), triplets for CH_2 (secondary carbons) and quadruplets for CH_3-groups. A 100.6 MHz 2-D ^{13}C-NMR spectrum recorded by this method is shown in Figure 6.44 for a neuraminic acid derivative. Parallel to the F_2-axis, the projection of the 2-D NMR spectrum represents the proton decoupled

^{13}C-NMR spectrum (shown at the upper edge of the 2D spectrum). Parallel to the F_1 axis, the multiplet structure of each signal is obtained. The multiplet structure makes it possible to decide which of the signals belongs to a CH_3, CH_2, CH, or to a quarternary carbon. The assignment of the signals is shown as it can be derived from the chemical shifts and the multiplet structure of the signal. From the separation of 2 lines in the multiplets, one can estimate half the value of the coupling constant ^1J(C,H). The contour diagram of the same spectrum is shown in Figure 6.45.

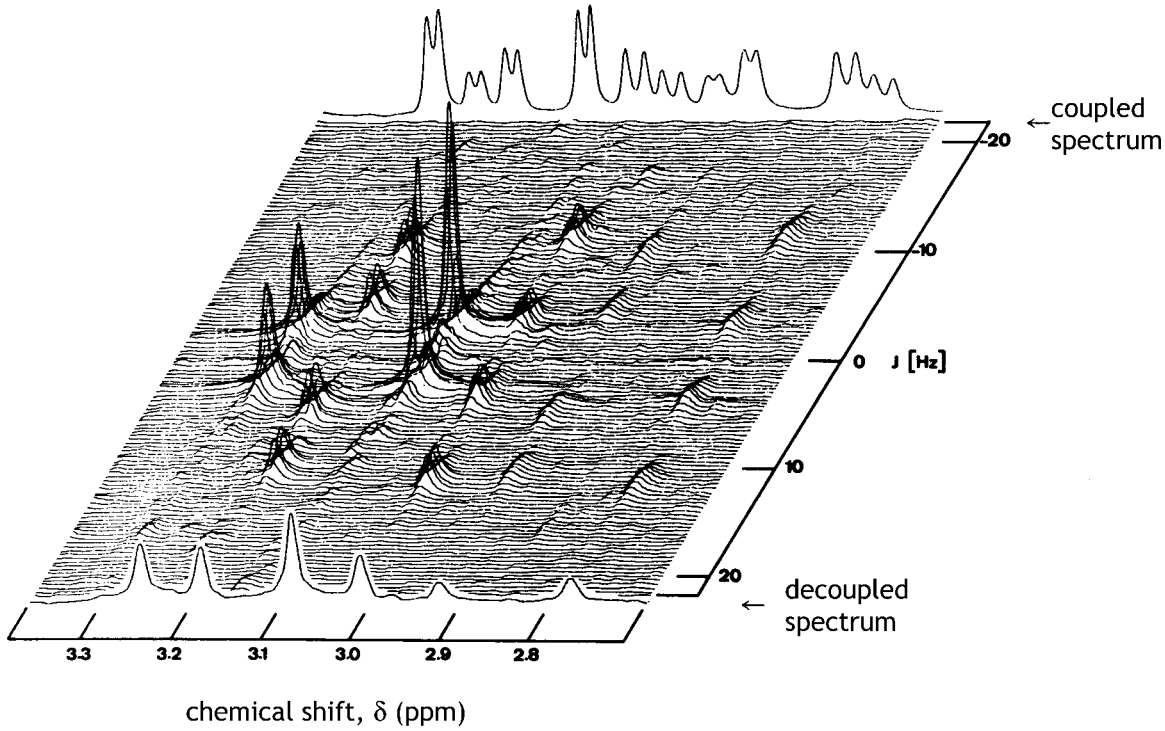

Part of the two-dimensional 360 MHz ^{1}H-NMR spectrum of a solution of the amino acids alanine, isoleucine, threonine, histidine and tryptophan. The non-decoupled spectrum is shown at the upper edge, the decoupled spectrum at the lower edge. The decoupled spectrum is the projection of the 2D spectrum along the J-axis.

Figure 6.46 Two dimensional J-coupled ^{1}H-NMR spectrum of a solution of different aromatic amino acids.

6.10.2 2-dimensional correlated spectroscopy.

6.10.2.1 Two-dimensional heteronuclear (H, C)-correlated NMR spectroscopy (H,C-COSY).

Many problems of signal assignment can be solved elegantly using the two dimensional chemical shift correlated spectroscopy (COSY). For a simple example, we again consider the two spin system of chloroform ($^{13}CHCl_3$) and perform an NMR experiment using the pulse sequence depicted in Figure 6.47 is used to obtain the spectrum. How the pulse sequence,

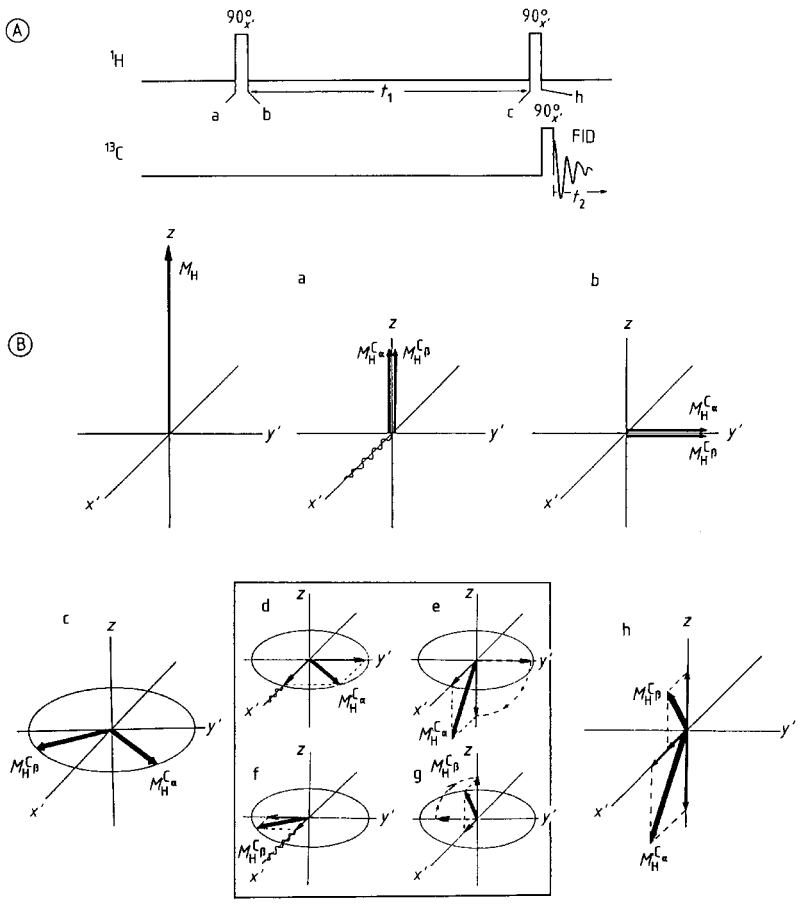

2-dimensional H, C-correlated spectroscopy. ***A*** pulse sequence. ***B*** vector diagrams that illustrate, how the ^{1}H magnetization vectors $M_H^{C\alpha}$ and $M_H^{C\beta}$ of an AX-two spin system (A=^{1}H and X=^{13}C) develop in a rotating coordinate system. The vector diagrams a to c correspond to the times given in ***A***. Diagrams d, e, f, and g depict the effect of the second $90°_x$ pulse separately for $M_H^{C\alpha}$ and $M_H^{C\beta}$ in the ^{1}H channel. The diagram h corresponds to the state in the ^{13}C channel before the $90°_x$ detection pulse.

Figure 6.47 2-dimensional H,C correlated NMR spectroscopy. A Pulse sequence. B Vector diagrams

$90°_{x'}$ — t1 —$90°_{x'}$, which is applied to the ^{1}H-channel, affects the macroscopic magnetization of the ^{1}H vectors, M_H^{Ca} and M_H^{Cb}, is shown in Figure 6.47 B. M_H^{Ca} and M_H^{Cb} correspond to the magnetizations of the chloroform molecules with ^{13}C in the α and in the β state. The first $90°_{x'}$ -pulse rotates both magnetization vectors from the z-axis to the y'-axis. In the following evolution phase, t_1, both vectors rotate with the Larmor frequencies

$$\nu_H - \frac{1}{2}J(\mathrm{C,H}) \qquad \text{and} \qquad \nu_H + \frac{1}{2}J(\mathrm{C,H}) \qquad \text{Eq. 6.34}$$

ν_H is the Larmor frequency without coupling, i. e. the resonance of the protons in $^{12}CHCl_3$. In the time t_1, M_H^{Ca} passes over the angle φ_α, M_H^{Cb} over the angle φ_β:

$$\varphi_\alpha = 2\pi\left(\nu_H - \frac{1}{2}J(\mathrm{C,H})\right)t_1 \quad \text{and}$$
$$\varphi_\beta = 2\pi\left(\nu_H + \frac{1}{2}J(\mathrm{C,H})\right)t_1 \qquad \text{Eq. 6.35}$$

The phase difference Θ is dependent only on the time t_1 and the coupling constant J(C,H):

$$\Theta = \varphi_\beta - \varphi_\alpha = 2\pi J(\mathrm{C,H})\, t_1 \qquad \text{Eq. 6.36}$$

For t_1=[4 J(C,H)]$^{-1}$: Θ = 90° and for t_2=[2 J(C,H)]$^{-1}$: Θ = 90°. In Figure 6.47 C, the status of the magnetization vectors is shown after an arbitrary time t1 (in the range of milliseconds). Since the frequencies of the 2 vectors do not coincide with the Larmor frequency of the rotating coordinate system, the vectors M_H^{Ca} and M_H^{Cb} are at an angle towards the y' axis. The vector M_H^{Ca} has components in the y' and in the x' axis. The second $90°_{x'}$ -pulse in the ^{1}H channel rotates the y'-component to the -z direction, while the x' remains unaffected. The new direction of the total magnetization M_H^{Ca} is determined by the components in x'-direction and in -z direction. In this example, the vector points to the lower front quadrant and is in the x', z -plane. The same observation is made for the y'-component of M_H^{Cb}: this component, however is transformed to the +z -direction, and M_H^{Cb} is found in the upper front quadrant in the x', z -plane. For further considerations, only the z-components of M_H^{Ca} and M_H^{Cb} are necessary. These longitudinal magnetizations are proportional to the populations differences between energy levels 1 and 3 (M_H^{Ca}) and between energy levels 2 and 4 (M_H^{Cb}). Two conclusions may be drawn: 1. By the pulse sequence $90°_{x'}$ — t_1 —$90°_{x'}$ the population ratios have changed compared to the initial state. The change in the population ratio is determined by t_1 and may even lead to a stronger population of level 3. 2. The state of the spin system depends on t_1 and on the angles φ_α and φ_β.. These angles are dependent on the Larmor frequency ν_H and on the coupling constant J(C, H).

How does the magnetization of the protons M_H that is induced by the pulse sequence in the ^{1}H-channel affect the ^{13}C-NMR spectrum ? The amplitude of the ^{13}C-NMR signal is determined by the population ratio after the second 90° pulse (compare the SPI experiment, section 6.9.3). The ^{13}C-NMR signal is not enhanced by a fixed factor, but is modulated as a function of t_1 by the Larmor frequencies of the protons. The magnetization vectors M_H^{Ca} and M_H^{Cb} — and therefore the signal intensities of the ^{13}C-NMR peaks — are affected to the same extent, but with opposite signs. The 90 $°_{x'}$ detection pulse in the ^{13}C channel rotates the longitudinal vectors to the +y‘ and –y‘ -axes. During the detection phase t_2, both vectors precess with the corresponding transition frequencies X_2 and X_1 and induce the interferogram in the detector.

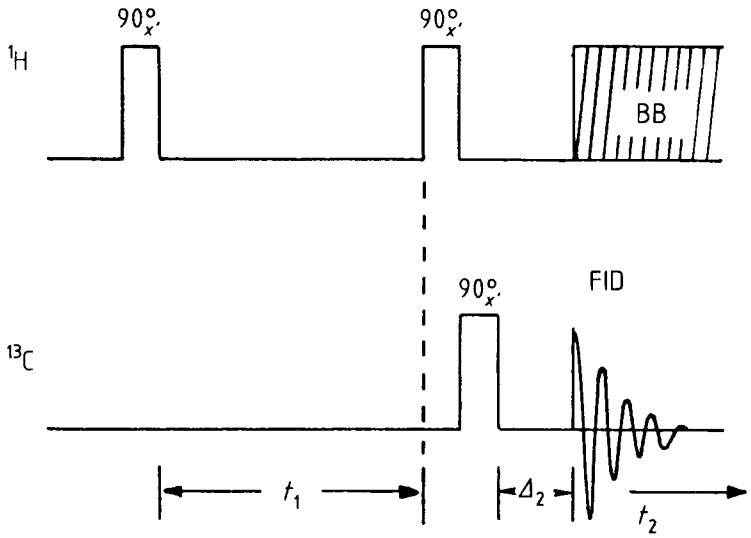

Extended pulse sequence to simplify the 2-dimensional H,C-correlated NMR-spectrum. After the 90°$_{x'}$ -pulse in the ^{13}C channel, a delay time Δ_2 is introduced, before the broad band decoupler is turned on and the FID is recorded.

Figure 6.48 Extended pulse sequence to simplify the H, C-COSY spectrum.

Fourier Transformation (FT) with respect to t_2 results in two signals on the F_2 axis, which are modulated by t_1 and by the resonance frequencies of the protons. If n spectra are recorded with different t_1 times and a FT is performed with respect to t_1, than a two-dimensional spectrum with 4 signals is obtained, two of which have a positive, the two others a negative amplitude. The F_1-axis describes the ^{1}H resonances and the F_2-axis the ^{13}C resonances. A and X are the frequencies of the corresponding transitions of ^{1}H and ^{13}C (which are usually given as δ values). The spectrum parallel to the F_2-axis corresponds to the coupled ^{13}C-NMR spectrum, the spectrum parallel to the F_1-axis corresponds to the coupled ^{1}H-NMR-spectrum.
In a simple spectrum, such as that of chloroform with only two coupled nuclei, spectra are still easy to interpret. For larger molecules, this experiment must be changed to reduce

complexity of the spectrum.

Unfortunately, one cannot simply turn on the broad band decoupler to reduce the carbon doublets to singlets, because the signals of interest would be destroyed (M_C^{Ha} and M_C^{Hb} have opposite signs, thus add up to zero). Only without BB-decoupling, two signals are found. A different state is observed, if we insert a delay time $\Delta_2 = [2\,J(C, H)]^{-1}$ between the $90°_{x'}$-detection pulse and the detection of the FID (Figure 6.48). During this time Δ_2 the faster magnetization vector M_C^{Hb} has progressed 180 ° more than M_C^{Hb} , and both vectors are again in phase, despite their differences in precession frequency. If the BB-decoupler is switched on in this moment, both vectors will precess equally fast. After FT of the FID with respect to t_2, only one signal is observed at ν_C. In a modified experiment, n spectra are obtained for different values of t_1, that are chosen to be equidistant with a difference of a few ms. The n ^{13}C NMR spectra are modulated by the proton resonance frequencies, according to the polarization transfer in the ^1H channel. After a second FT with respect to t1, the 2-dimensional spectrum is obtained that consist now of 2 signals that correspond to one transition of ^{13}C and two transitions of ^1H.

Finally, we can use the pulse sequence depicted in Figure 6.49 to reduce the two resonance lines to one single signal. New is a 180° pulse in the ^{13}C channel after exactly $t_1/2$ ms and a delay time Δ_1 before the second pulse in the ^1H channel. The vector diagram in Figure 6.49 B, illustrates the experiment. The first 90 ° pulse rotates the two ^1H magnetization vectors M_H^{Ca} and M_H^{Cb} to the y'-axis. According to their Larmor frequencies, $\nu_H - J(C, H)/2$ and $\nu_H + J(C, H)/2$ there is a different precession of the two vectors. After time $t_1/2$, the phase difference between the vectors is $\Theta = \pi J(C, H)\, t_1$. By a 180 ° pulse in the ^{13}C-channel α-^{13}C nuclei become β- ^{13}C nuclei and vice versa. This means, M_H^{Ca} becomes M_H^{Cb} and M_H^{Cb} becomes M_H^{Ca} . Now the faster vector is behind the slower vector in the vector diagram (thick and thin arrow). After another time $t_1/2$ ms the faster vector has reached the slower vector and both are in phase. The total angel φ that the vectors have passed is only dependent on the Larmor frequency of the protons (without coupling with the ^{13}C nuclei). A pulse that would directly follow after time t_1 would not result in a polarization of the ^{13}C NMR signal. However if a delay time of Δ_1 is introduced before the second pulse $90°_{x'}$ in the ^1H-channel, the vectors M_H^{Cb} and M_H^{Cb} have progressed again by different angles that have a difference of 180 ° after $\Delta_1 = [2\,J(C, H)]^{-1}$ ms. A $90°_{x'}$ pulse in the ^1H channel causes the y' -components of the vectors to rotate to the -z and +z directions, and therefore the induction of polarization. How large this polarization is, depends on the angle φ. If both vectors are positioned along the y'-axis, the polarization has a maximum. If they are positioned along the x'-axis, the polarization is zero. The angle φ, by which the vectors have progressed, is a function of the Larmor frequency ν_H of the decoupled protons. The evolution of the spin system continues during the time Δ_1, but this time is a constant among all spectra that are collected with different times t_1. The state of polarization that affects the intensities of the ^{13}C resonances, is therefore exclusively determined by the Larmor frequency ν_H of the protons. The subsequent events in the experiment

are a 90° pulse in the 13C channel, which rotates the magnetization vectors M_C^{Ha} and M_C^{Hb} in the +y' and the -y' directions. After a constant time $\Delta_2 = [2\ J(C, H)]^{-1}$ ms these vectors are again in phase. In this moment, the BB-decoupler is turned and it will stop the coupling between ^{13}C and ^{1}H. The first Fourier transform with respect to t_2 results in a signal at ν_C. If spectra were recorded with different times t_1 and with $\Delta_1 = \Delta_2 = [2\ J(C, H)]^{-1}$ ms then the signal intensities are modulated with ν_H. A second Fourier transform with respect to t_1 results in a two-dimensional spectrum (F_1, F_2) which consists of only one signal with the coordinates (ν_1, ν_2).

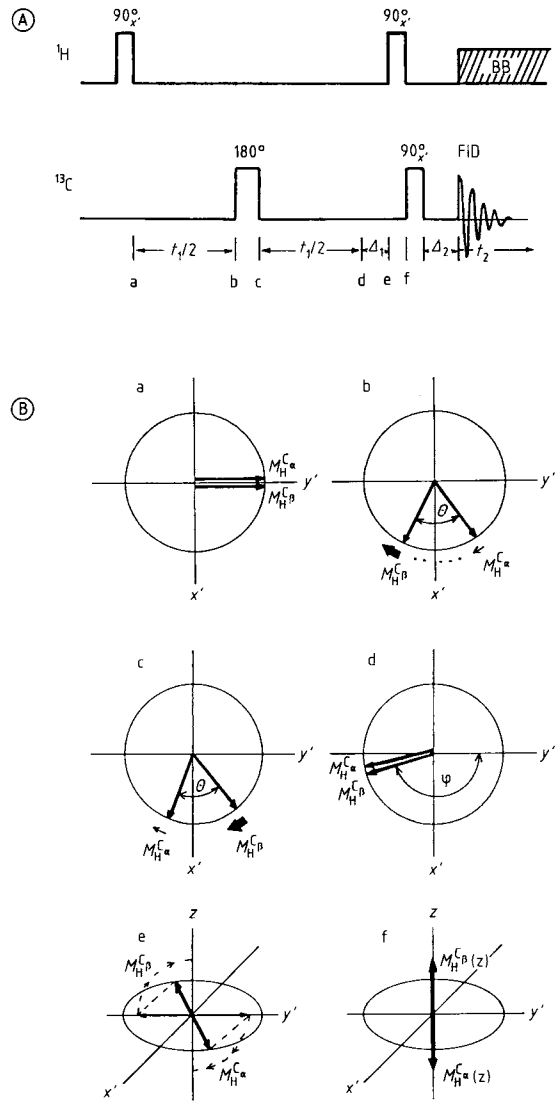

A. Pulse Sequence for a 2-dimensional H,C-correlated NMR experiment in which the 2D spectrum of a AX Twospin system is reduced to one signal.
B. Vector diagrams illustrate the positions of the ^{1}H-magnetization vectors $M^{H}C_{\alpha}$ and $M^{H}C_{\beta}$ and their z-components at the times given in A. In diagrams a through d only the x-y plane is depicted.

Figure 6.49 Pulse sequence for the 2-dimensional H, C -correlated experiment.

The signal is most intense for $\Delta_1 = [2\ J(C, H)]^{-1}$ ms. Furthermore, signal intensity is amplified by transfer of magnetization from the more sensitive ^1H nucleus to the less sensitive ^{13}C nucleus. The time period between the end of t_1 and the beginning of t_2 is called "mixing". The same experiment can be performed for multi-spin systems.

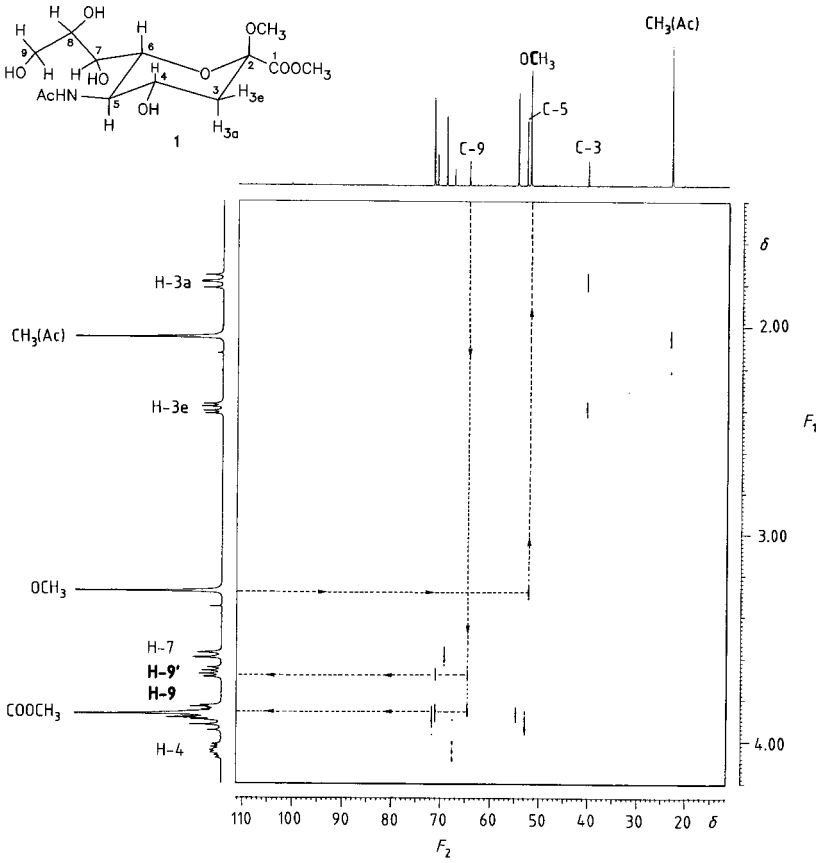

2-dimensional H,C correlated 100.6 MHz-NMR spectrum of a neuraminic acid derivative. On the left, the 1-dimensional ^1H-NMR spectrum is shown, and above, the projection of the 2-dimensional NMR spectrum to the F_2-axis, the ^{13}C-NMR spectrum, is depicted.

Figure 6.50 2-dimensional H,C -correlated 100.6 MHz NMR spectrum of a neuraminic acid derivative. The spectrum was recorded in D_2O.

Figure 6.50 shows the 2-dimensional H,C correlated 100.6 MHz NMR spectrum of a neuraminic acid derivative. On the upper edge, the 1-dimensional (1-D) ^{13}C-NMR spectrum is shown. This spectrum is obtained by projecting the 2-D peaks to the F_2-axis. Those signals can be recognized that are directly connected to ^1H-atoms. The three quarternary carbons do not appear as correlation peaks. On the left hand side, the 1-dimensional ^1H-NMR spectrum is shown. By characteristic chemical shifts and multiplicities, a few assignments are clearly defined. In the 1H-NMR spectrum, these are the assignments of the three methyl signals and also those of H-3a, H-3e, and possibly H-4 and H-7. In the 1-D ^{13}C-NMR spectrum, the

resonances of the methyl carbon of the NAc-group and C-3, C-5, C-9 are known. Known are also the chemical shifts of the two O-CH_3 signals, but they cannot be assigned unambiguously. For analysis we start with the assigned signals of the ^{1}H resonances. The correlation peaks in the 2-D spectrum now give us the chemical shifts of connected carbon atoms in the 1-D ^{13}C NMR spectrum. In addition to the already known resonances, we can now assign the chemical shifts of the two methoxy groups as well as those of C-4 and C-7.

If we start the analysis with the assigned ^{13}C resonances, we are now able to assign the chemical shifts of H-5, H-9, and H-9‘, in addition to those ^{1}H-nuclei, that were assigned on the basis of the ^{1}H-NMR spectrum alone. For C-3 and C-9 we obtain two correlation peaks, because these C-atoms are bound to two diastereotopic H-atoms.

With the new assignments, the NMR spectrum, the 1-dimensional ^{1}H and the ^{13}C NMR spectra are almost completely analyzed. Only the assignments of H-6 and H8, and C-6 and C-8 are missing. This assignment cannot be made on the basis of the (H,C)-correlated 2-D NMR spectrum, since resonances are too close in both the ^{13}C and the ^{1}H-NMR spectrum. The results are summarized in Table 5 .

basis for assignment	assignment
H-4	C-4
H-7	C-7
OCH3 (ketosid)	OCH3
OCH3 (ester)	OCH3
C-5	H-5
C-9	H-9
C-9	H-9‘

Table 5 Results of the analysis of the (H, C) COSY 2D-NMR spectrum

The COSY method is widely used in the analysis of large molecules, such as those found in biochemistry and natural substances. A major advantage is that the relatively large chemical shifts of the ^{13}C nuclei can be combined with those of the ^{1}H nuclei.

6.10.2.2 Two-dimensional homonuclear (H, H)-correlated NMR spectroscopy (H,H-COSY).

The 2-dimensional homonuclear (H,H)-correlated NMR experiment results in spectra that contain ^{1}H chemical shifts on both frequency axis. This method became known as correlated spectroscopy (COSY). It is based on the pulse sequence $90°_{x'}$ — t_1 —$\Theta_{x'}$ (Figure 6.51).

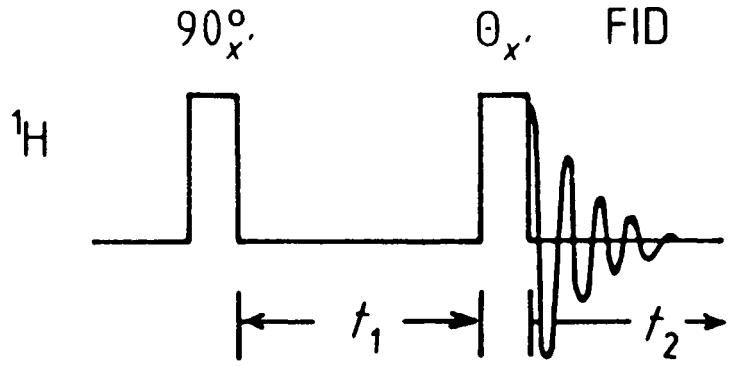

Pulse-Sequence for a 2-dimensional homonuclear (H,H)-correlated NMR experiment (COSY). The variable is t_1. $\Theta = 90°_{x'}$ or $45°_{x'}$, sometimes $\Theta = 60°_{x'}$.

Figure 6.51 Pulse sequence for the 2-dimensional homonuclear (H,H)-correlated NMR experiment (COSY).

We shall consider the experiment for an AX two spin system with a second pulse of $\Theta_{x'}$ = 90°. A and X are ^{1}H nuclei with a coupling constant of J(A,X). The pulse sequence therefore is $90°_{x'}$ — t_1 —$90_{x'}$. In contrast two the heteronuclear C,H-COSY experiment, there is an important difference: the first pulse $90°_{x'}$ affects the magnetization vectors of both the A and X nuclei, M_A and M_X, which are rotated to the y'-axis. Because of the coupling J(A,X) there are two macroscopic magnetization vectors, $M_A^{X\alpha}$ and $M_A^{X\beta}$, depending on the state of the X nucleus, which maybe an α or a β -state. Similarly, we must also consider two Mx vectors, $M_X^{A\alpha}$ and $M_X^{A\beta}$. These vectors rotate in the x, y -plane with the frequencies $\nu_A \pm J(A,X)/2$ and $\nu_X \pm J(A,X)/2$ around the z-axis. Within the time t1, which is the variable in the COSY experiment, the 4 magnetization vectors will separate within the x, y -plane because of their different frequencies. After a time t_1, each of the four vectors has a component in x' and in y' direction. The following second $90°_{x'}$ -pulse rotates the y' -component to the z axis, either in –z or in +z direction. This step includes a polarization transfer (compare section 6.9.3) To which extent magnetization is transferred, depends on the state of the spin system at time t_1, and therefore on the Larmor frequencies ν_A, ν_x and on the coupling constant J(A,X). The x'- components of the magnetization vectors, which are also dependent on the evolution of the spin state and which continue to rotate in the x', y' -plane, result in a free

induction decay, which after FT with respect to t_2, yield a four line AX spectrum with the frequencies:

$$\nu_A + \frac{1}{2}J(\mathrm{A,X}) \qquad (\mathrm{A}_1) \qquad \nu_A - \frac{1}{2}J(\mathrm{A,X}) \qquad (\mathrm{A}_2)$$
$$\nu_\mathrm{X} + \frac{1}{2}J(\mathrm{A,X}) \qquad (\mathrm{X}_1) \qquad \nu_\mathrm{X} - \frac{1}{2}J(\mathrm{A,X}) \qquad (\mathrm{X}_2)$$

These frequencies correspond to the transitions A_1, A_2, X_1, X_2 that are depicted in Figure 6.39. The signals are modulated as a function of t_1 with the these four frequencies. The second Fourier transform with respect to t_1 therefore leads to a two-dimensional spectrum with four groups that each contain 4 signals. Two of these groups are centered around ν_A, ν_A and ν_X, ν_X, the diagonal peaks. The other two are centered around ν_A, ν_X and ν_X, ν_A, the so called correlation peaks or cross peaks. Diagonal and crosspeaks form the corners of a square. *The important feature of the 2-D spectrum is that the correlation peaks (cross peaks) are always found when two nuclei are coupling by j-coupling.* Within each group the signals are separated

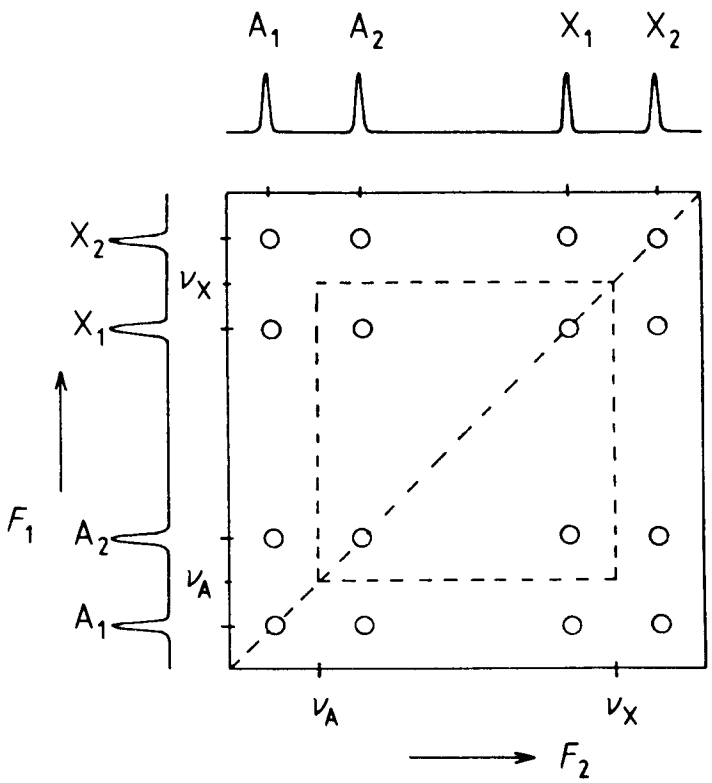

Scheme of a COSY spectrum of a AX two spin system with A=X=H. Shown are absolute values. In a real spectrum, signals on the diagonal are dispersion signals that may also have a negative amplitude. The diagonal peaks and the cross peaks of coupling nuclei form the corners of squares.

Figure 6.52 Scheme of a homonuclear COSY spectrum.

by the coupling constant J(A,X) in each dimension (F_1-axis and F_2-axis). The projection of the COSY spectrum in each dimension F_1 or F_2 corresponds to the 1-dimensional ^{1}H-NMR spectrum (Figure 6.52). Figure 6.52 shows the 2D homonuclear COSY spectrum in form of a contour plot schematically with the absolute values of the signals.

If a proton couples with more than one neighboring proton, then the diagonal peak is found in the corner of more than one square. In this way, the chemical shifts of coupled nuclei can be determined even in complex spectra. Therefore, the COSY experiment is an important tool in the assignment of ^{1}H resonances. It is superior to the 1D NMR experiment and various decoupling experiments, because the relations and chemical shifts between all coupling nuclei are obtained at once, with a single experiment.

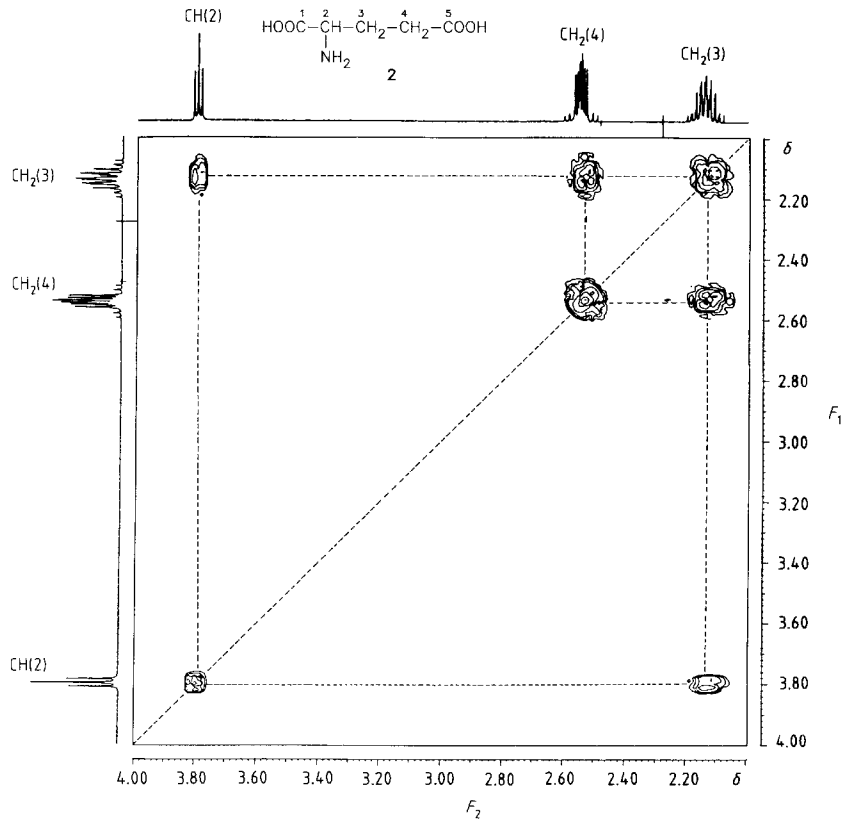

500 MHz COSY-90 spectrum of glutamic acid. On the upper and on the left edge, the 500 MHz 1-dimensional ^{1}H-NMR spectra are shown. The dashed lines connect the diagonal and the correlation peaks, which indicate the protons that couple by scalar coupling. The diagonal peak of the C-3 protons is located in the corner of two squares, since these protons couple with the protons on C-3 and on C-4.

Figure 6.53 500 MHz COSY spectrum of glutamic acid.

Figure 6.53 shows the (H,H) COSY-90 spectrum of glutamic acid. On the left and on the upper edge, the 1-dimensional ^{1}H NMR spectra are shown. On the diagonal, three multiplets are observed, which correspond to the three multiplets of the one-dimensional spectrum. With these multiplets and the correlation peaks it is clear which of the protons are coupling. Since the protons on C-3 couple with the protons on C-4 and with the protons on C-2, the multiplet of the C-3 protons is found in the common corner of two squares. By a suitable choice of experimental conditions, even far reaching smaller coupling can be detected. A disadvantage of the method is, that in larger molecules the COSY contour diagram can easily be too crowded. If there are only minor differences in the chemical shifts of coupling nuclei,

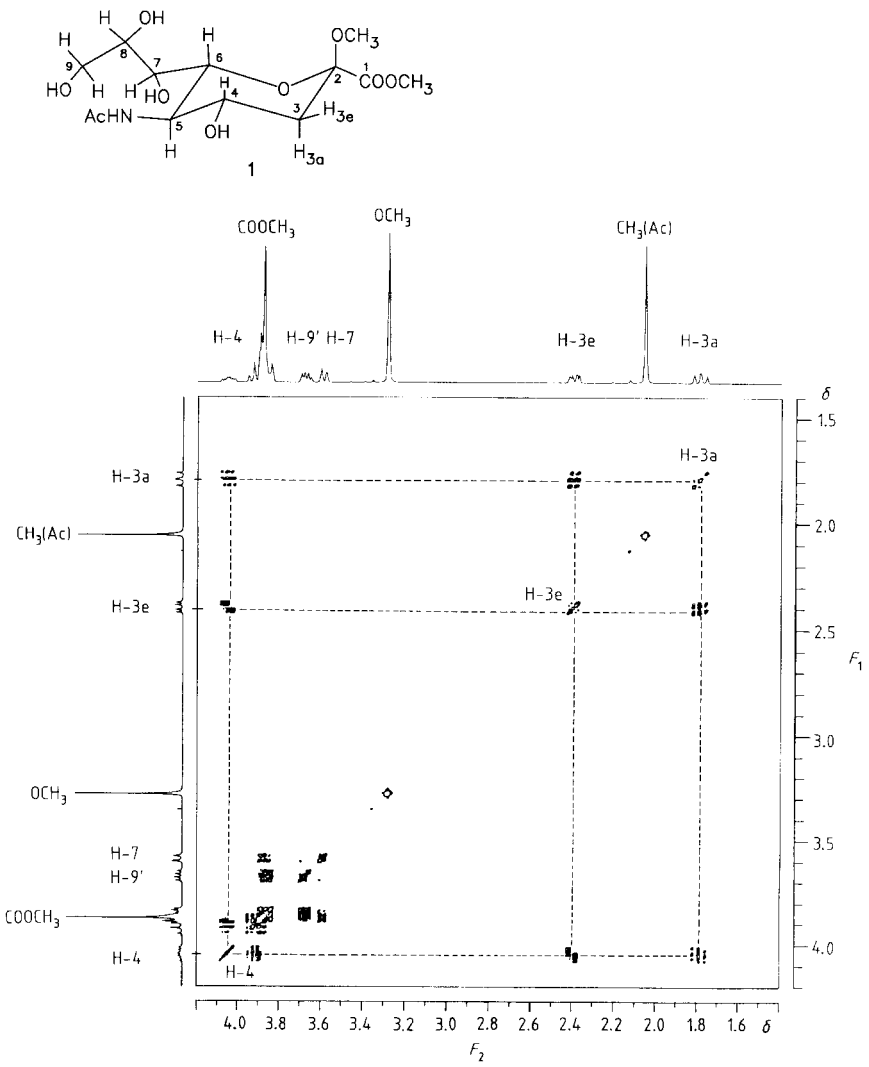

400 MHz-COSY-45 spectrum of a neuraminic acid derivative. Above the 2D-spectrum, the projection of the 2D-spectrum to the F_2-axis is shown. On the left hand side, the projection of the 2D-spectrum to the F_1-axis is the ^{1}H-NMR spectrum. (20 mg of the substance were used in 0.5 mL D_2O. Data acquistion time was 15.4 hrs).

Figure 6.54 400 MHz (H, H) -COSY spectrum of neuraminic acid.

then the coupling nuclei may be difficult to identify.

If $\Theta_{x'}$ is chosen to be smaller than $90°_{x'}$, the spectrum is simplified. The magnetization is transferred preferentially, such that some signals among the diagonal or correlation peaks are weaker than others. A smaller angle has the disadvantage that the sensitivity is reduced. A fair compromise is an angle of 45 ° (sometimes maybe 60°).

As an example we consider the 400 MHz (H,H)-COSY spectrum of neuraminic acid. Figure 6.54 shows the 400 MHz homonuclear (H, H)-COSY-45 spectrum of neuraminic acid in the region of δ = 1.4 to 4.2 ppm. The section from δ = 3.4 to 4.2 is depicted in enlarged form in Figure 6.55. Projections of the peaks to the F_2 -axis are given at the upper edge of the 2-D spectrum and the 1-dimensional ^{1}H-NMR spectrum is given on the left side of the 2-D spec-

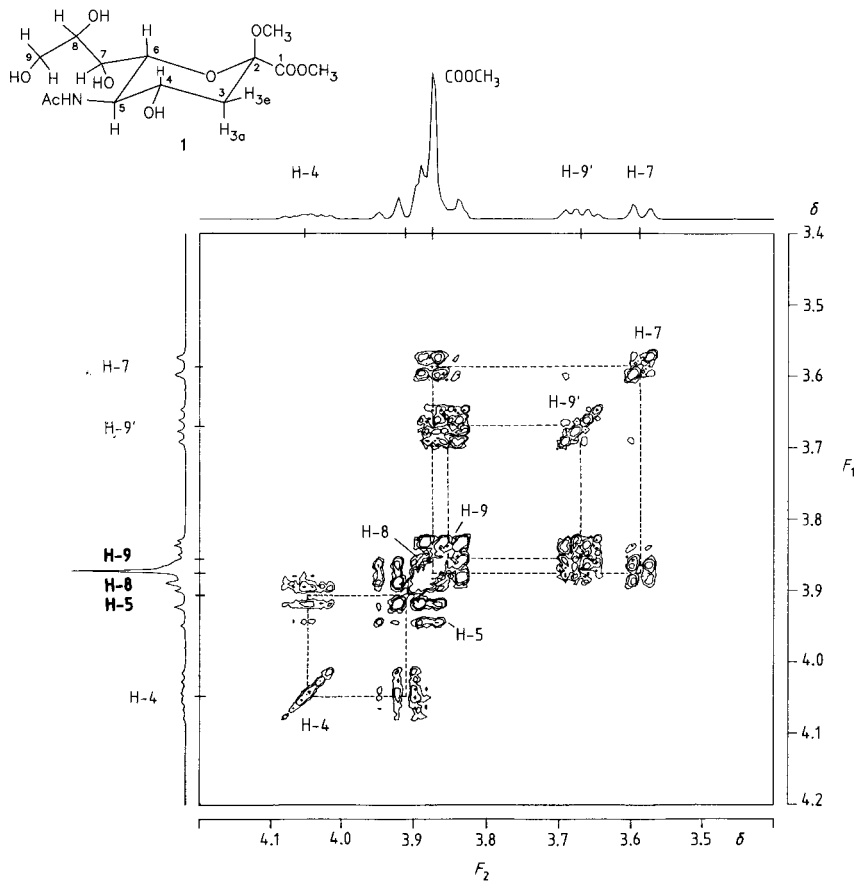

Enlarged part of the spectrum of a neuraminic acid derivative. With the signals of protons H-4, H-7, and H-9' that are given in the upper 1D spectrum, it is possible to locate the signals of H-5, H-8, and H-9 by analysis of the correlation peaks.

Figure 6.55 Enlarged section of the homonuclear (H, H)-COSY-45 spectrum of neuraminic acid shown in Figure 6.54

trum. To analyze the 2-D spectrum, we connect the diagonal and the crosspeaks (correlation peaks) to form squares. Beginning with the unambiguous assignments of the H-3a and H-3e protons, the correlation peaks can be used to find the chemical shifts of the neighbor protons, which is the H-4 multiplet at δ = 4.0 to 4.05. This multiplet forms the corner of another square (Figure 6.55), by which the chemical shift of H-5 can be identified. Since the difference of the chemical shifts between H-5 and H-6 is small, it is difficult to determine the corresponding square. The analysis is preferably continued with another unambiguous signal, H-7, which shows a doublet at δ = 3.6. The correlation peaks lead to a coupling nucleus, which can be H-6 or H-8. We cannot easily distinguish between these nuclei. However, it is known by other experiments that the coupling constant J(H-6, H-7) is small. The correlation peak therefore points to H-8. From H-8 we can find the shift of H-9' and H-9.

The example demonstrates that we need some clearly assigned peaks to start the interpretation of the 2-D (H, H) COSY experiment. In this example, the assignments of the peaks of H-3 and H-7 were used as a start. The signals of the other protons could be identified with the exception of some uncertainty in the section of δ = 3.85 to δ = 3.95, since in this region the multiplets of H-5, 6, 8, 9, and the methyl signal of the ester are superimposed. Another result is that non-coupling protons, in this case those of the methyl groups, only exhibit signals on the diagonal.